Masses of the unbound nuclei ^{16}Ne, ^{15}F, and ^{12}O

G. J. KeKelis,* M. S. Zisman, D. K. Scott, R. Jahn,‡ D. J. Vieira, and Joseph Cerny
Department of Chemistry and Lawrence Berkeley Laboratory, University of California, Berkeley, California 94720

F. Ajzenberg-Selove
Department of Physics, University of Pennsylvania, Philadelphia, Pennsylvania 19174
(Received 20 October 1977)

The (^{4}He,^{8}He) and (^{3}He,^{8}Li) reactions have been employed at detection angles near 8° on gas targets of ^{20}Ne and ^{16}O to produce and measure the masses of the nuclei ^{16}Ne, ^{15}F, and ^{12}O. The (^{4}He, ^{8}He) reactions were performed at an incident energy of 117 MeV and the (^{3}He, ^{8}Li) reaction at 88 and 75 MeV. The mass excesses of ^{16}Ne, ^{15}F, and ^{12}O were determined to be 23.92 ± 0.08, 16.67 ± 0.18, and 32.10 ± 0.12 MeV, respectively. Estimated ground state decay widths were $\Gamma_{c.m.} = 0.2 \pm 0.1$, 0.8 ± 0.3, and 0.40 ± 0.25 MeV, for ^{16}Ne, ^{15}F, and ^{12}O, respectively. A d coefficient of 8 ± 5 keV is indicated for the isobaric multiplet mass equation description of the mass 16 multiplet. Consideration of the possible decay mechanisms of ^{16}Ne and ^{12}O indicates that both nuclei probably have an appreciable diproton decay width.

[NUCLEAR REACTIONS ^{20}Ne(^{4}He,^{8}He), ^{16}O(^{4}He,^{8}He), ^{20}Ne(^{3}He,^{8}Li). Measured reaction Q values, ground state $\Gamma_{c.m.}$; deduced mass excesses. Deduced coefficients for IMME. Discuss diproton decay widths.]

I. INTRODUCTION

Increasing sophistication in detection systems for large solid-angle spectrometers, coupled with high energy and high beam intensity cyclotrons, has proven advantageous in the study of very low cross section reactions which are designed to measure accurately the masses of nuclei far from stability. In particular, utilization of the (^{4}He, ^{8}He) and (^{3}He,^{8}Li) reactions has been productive in investigations of the neutron deficient light nuclei with $T_z = -2$ and $-\frac{3}{2}$.[1-4] Results of investigations such as these have been used to test various mass relations. One such relation, the isobaric multiplet mass equation (IMME),[5] has been shown to provide a particularly accurate description of the mass excesses of an isobaric multiplet. Near the limit of stability, as nuclei become unbound, one might expect that mass relations could fail, but the IMME appears to work well even for unbound nuclei.[1,6]

In this paper we present the results of an investigation, using the reactions mentioned above, designed to measure the masses of ^{16}Ne, ^{15}F, and ^{12}O, all of which are predicted to be unbound to proton emission. At the outset of this experiment the masses of the $T = 2$ ground states of ^{16}Ne and ^{12}O could be estimated using the IMME since three members from each of the mass 16 and 12 multiplets were known.[7-10] The mass of ^{15}F was obtained from a Kelson-Garvey prediction.[11] None of these nuclei had been observed at the start of this investigation.[12,13]

The masses of these nuclei are of particular interest since ^{16}Ne and ^{12}O have long been candidates for nuclides decaying by the prompt emission of a pair of protons.[14] Of course, this "diproton" emission must compete with the sequential emission of two protons unless the parent nucleus is bound to emission of a single proton. For the particular case of ^{16}Ne, the diproton emission to ^{14}O must compete with sequential proton emission first to ^{15}F and then to ^{14}O. The relative widths for the two decay processes are partially determined by the penetrabilities of the emitted protons, and diproton emission can compete only if the single proton is barely unbound. Therefore, the masses and widths of both the ^{16}Ne and ^{15}F ground states must be determined in order to permit an evaluation of the penetrabilities.

II. EXPERIMENTAL PROCEDURE

Beams of 88 and 75 MeV ^{3}He^{+2} and 117 MeV ^{4}He^{+2} particles at intensities of ~150 nA were obtained from the Lawrence Berkeley Laboratory 88-inch cyclotron. After passing through two dipole magnets for energy analysis, the beam entered the scattering chamber, impinged on a gas target, and was stopped in a water-cooled split Faraday cup. Placement of the Faraday cup inside the scattering chamber allows measurements to be made at detection angles as small as 2.5°. To complement this capability, a gas target and associated collimation system were designed to operate at angles less than 10°. Using ^{20}Ne and ^{16}O gases (enriched to >99.5%), the effective target thicknesses were 1.2 ± 0.4 and 1.9 ± 0.6 mg/cm^2, respec-

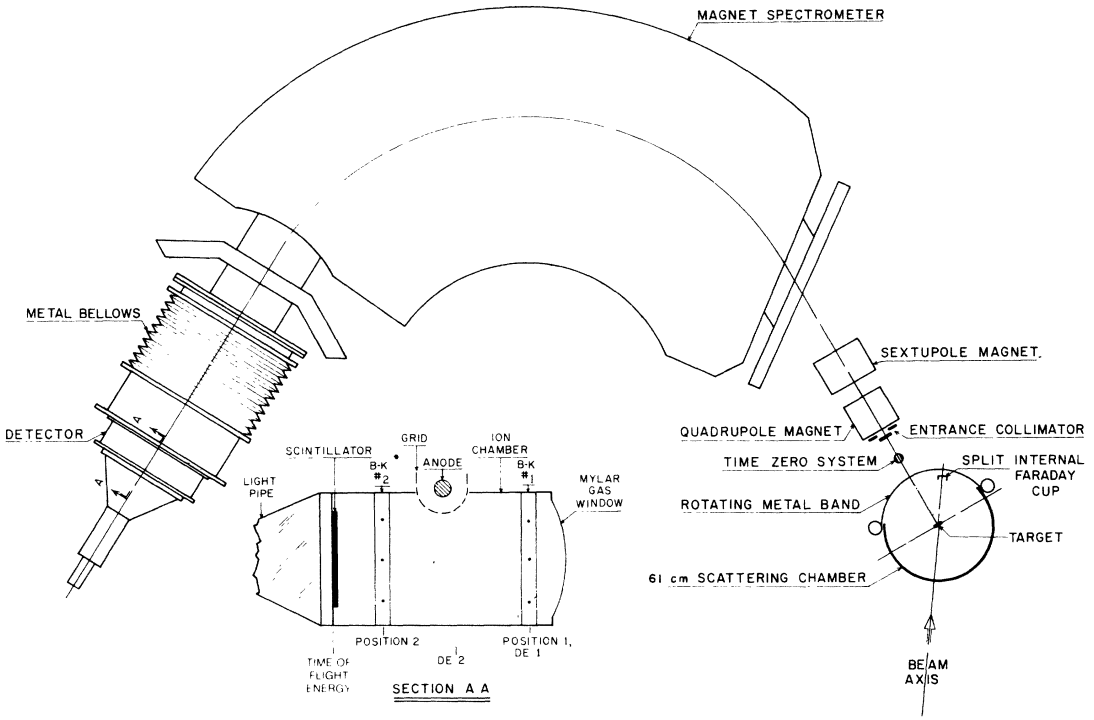

FIG. 1. The quadrupole-sextupole-dipole spectrometer and side view of the focal plane detection system.

tively, at a gas pressure of 310 Torr. Entrance and exit foils of the gas target were constructed from 1.98 ± 0.14 mg/cm^2 thick HAVAR.

Emitted reaction products were accepted into a 2 msr solid angle and passed through a time-zero detector located at the exit of the scattering chamber as shown in Fig. 1. This detector was a parallel plate gas counter[15,16] consisting of three electrodes and two gas containment windows. The outer two electrodes were ground planes and were spaced at a distance of 1.0 cm from the central electrode which operated at + 950 V and served as the collection anode. Operating with propane gas at a pressure of 10 Torr, the total detector thickness was 1.77 ± 0.13 mg/cm^2. When a charged particle passed through the counter, the resulting electron cascade produced a fast negative signal ($\tau_R = 20$ ns) at the anode which was suitable for fast timing. This counter operated efficiently at count rates exceeding 500 kHz and was insensitive to the large γ and neutron flux produced at the Faraday cup.

After passing through the time-zero detector, particles emitted from the target were collimated and magnetically analyzed in a quadrupole-sextupole-dipole (QSD) spectrometer.[17] Particle identification was performed on those particles reaching the focal plane using the detection system shown in Fig. 1.[18] Two position measurements (POS1 and POS2) were obtained in 1.0 cm thick Borkowski-Kopp proportional counters and were combined to provide trajectory (ANG) information. Differential energy loss, which for a given value of $B\rho$ is proportional to $(MZ/Q)^2$, was measured in a 10 cm thick ion chamber ($\Delta E2$) as well as in the first Borkowski-Kopp detector ($\Delta E1$), and the residual particle energy (E), which is proportional to Q^2/M, was measured with a plastic scintillator coupled to a photomultiplier. Fast signals obtained from the anodes of the photomultiplier and the time-zero detector were combined to yield a time-of-flight measurement (TOF) over the 7 m flight path. For a given value of $B\rho$ the time of flight is proportional to M/Q. Finally, the vertical position (VERT) of an event was obtained by comparing the drift time of the electrons produced in the ion chamber to the relatively instantaneous anode signal from the photomultiplier. Eight parameters (POS1, POS2, $\Delta E1$, $\Delta E2$, E, TOF, VERT, and ANG) were available for display on line and were event recorded on magnetic tape for later analysis.

The focal plane detector, which has a total length of 45 cm, was collimated to 12 cm in the (^{4}He, ^{8}He) experiments because of the high counting rates which were encountered. Lead and paraffin were used to shield it from the intense background radiation produced

TABLE I. Ground state error analysis. All error contributions are given in keV.

	^{16}Ne	^{15}F	^{12}O
Beam energy (±0.05%)	23	18	27
Detection angle (±0.15°)	13	10	15
Focal plane calibration error (rms)	13	20	18
Spectrometer drift (±0.006%)	7	8	8
Uncorrelated thickness uncertainty in gas target and time-zero detector (±5%)	43	113	72
Centroid uncertainty	51	125	86
^{8}He and ^{8}Li mass [a]	12	2	12
Total	~80	~180	~120

[a] Reference 10.

at the Faraday cup.

When taking data with the (^{4}He, ^{8}He) reaction it is advantageous to choose a beam energy which is high enough to make the rigidity of the emitted ^{8}He particles greater than that of the elastic ^{4}He particles. This greatly reduces the counting rate since no elastic or inelastically scattered particles need be incident on the detector. The required energies for the (^{4}He, ^{8}He) reactions on targets of ^{20}Ne and ^{16}O are 124 and 138 MeV, respectively, and approach the upper energy limit of the 88-inch cyclotron. Therefore, the experiments to measure both the ^{16}Ne and ^{12}O masses were performed at a somewhat lower beam energy of 117.4 MeV. Although inelastically scattered α particles were then incident on the focal plane detector, the detection system described above was capable of reliably observing one ^{8}He particle in more than 10^{7} incident charged particles.

When measuring the mass of a nuclide using this experimental approach, errors in the mass assignment must reflect the uncertainties in the values of the following parameters: beam energy, detection angle, target and time-zero detector thicknesses, calibration errors, centroid uncertainties, and the mass of the detected particle. The procedures used to determine the uncertainties in these parameters will now be presented. (See also Table I.)

The beam energy was determined from the absolute calibration of the energy analyzing magnets, which was checked with the ^{12}C+p resonance at 14.231 MeV.[19] The uncertainty in the energy was conservatively taken as ±0.05%. The reaction scattering angle was determined optically to an accuracy of ±0.05° and the 2 msr solid angle corresponded to a horizontal acceptance angle of 1.1°.

Particular care was taken to minimize the uncertainty arising from the large energy losses in the gas target and time-zero detector since these were potentially the largest sources of error in the mass measurement. Thicknesses of the containment windows of the gas target and foils in the time-zero detector were determined directly by weighing and indirectly from the energy loss of 8.78 MeV α particles. An additional measurement of the thickness of the time-zero detector was obtained by observing the energy shift of ^{6}He particles, produced in the ^{20}Ne(^{4}He, ^{6}He)^{18}Ne reaction, with and without the time-zero detector. Similar checks of the target thickness were performed by observing energy shifts of the ^{6}He particles as a function of target gas pressure. Finally, the effective target thickness was calculated from the known geometry and was also checked by comparing the yield of elastic scattering from a ^{12}C target foil of known thickness to that obtained from filling the gas target with propane. The final thickness of each component was obtained by taking a weighted average of all the measurements and each was determined to an accuracy of about ±7%.

In order to determine the masses of the nuclei of interest, the rigidities of the emitted ^{8}He or ^{8}Li particles were compared to the known rigidities of particles from two other reactions. For the (^{4}He, ^{8}He) reactions, ^{4}He elastic or inelastic scattering and the (^{4}He, ^{6}He) reaction were used to calibrate the focal plane detector, while for the (^{3}He, ^{8}Li) reaction, ^{3}He elastic and inelastic scattering and the (^{3}He, ^{6}Li) reaction were employed. For both the ^{3}He and ^{4}He induced reactions a straight-line fit for ρ versus channel was obtained for all the calibration points and the resulting average root-mean-square deviation was taken as the error in the calibration. As a final check on both the consistency of the calibration and the detector resolution, α particle inelastic scattering on ^{20}Ne (leading to states at 5.79 and 7.18 MeV) and the ^{20}Ne(^{3}He, ^{6}Li)^{17}F reaction (leading to the ground and first excited state of ^{17}F) were detected on the focal plane simultaneously with the reactions of interest.

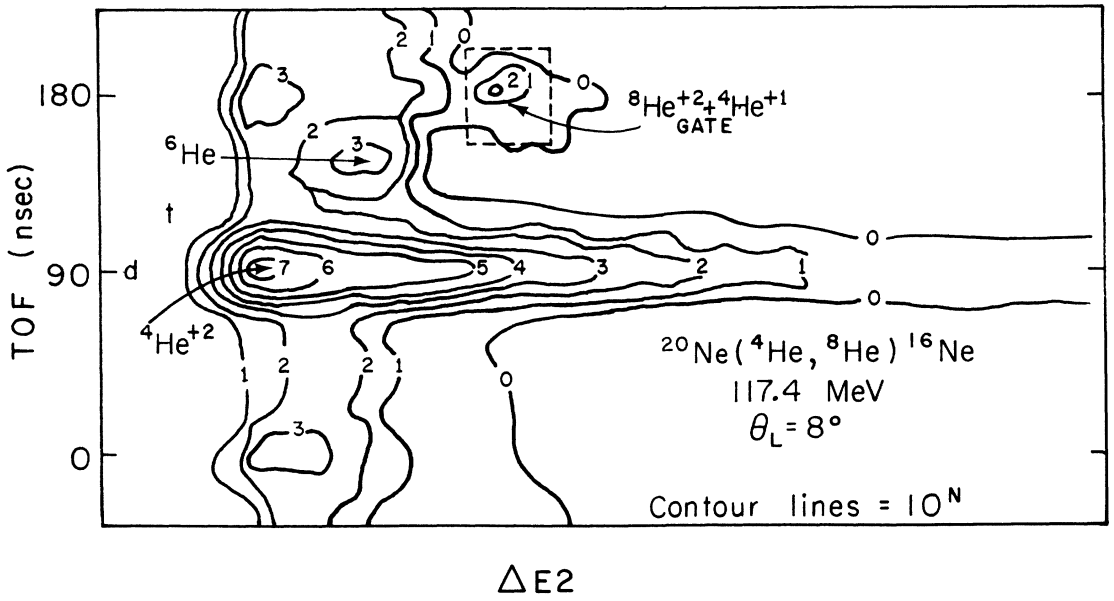

FIG. 2. Ungated (relative) time-of-flight vs differential energy loss contour plot for the ^{20}Ne(^{4}He,^{8}He)^{16}Ne reaction. The proton, deuteron, triton, and α particle groups were gated out during the experiment, but the α particle group has been simulated for display purposes. Numerals indicate 10^{N} counts, with 10^{0} being the furthest excursion of scattered single counts. The particle group at 180 nsec and above the ^{4}He^{+2} group is due to pileup and the group at 0 nsec and below the ^{4}He^{+2} group is due to less than 100% efficiency in the time-zero detector.

III. RESULTS

A. ^{20}Ne(^{4}He,^{8}He)^{16}Ne

This experiment was performed at two slightly different bombarding energies. An ungated contour plot of time-of-flight versus differential energy loss in the ion chamber detector, taken at an incident energy of 117.4 MeV and $\Theta_L = 8°$, is shown in Fig. 2. The p, d, t, and ^{4}He particle groups were excluded with a lower level discriminator in order to reduce the data accumulation rate. A well-defined group is present at the expected location of the ^{8}He particles. Although no discrimination can be made between ^{8}He^{+2} and ^{4}He^{+1} particles in this display, there is excellent separation from all other particle species. The residual energy measurement from the light output in the plastic scintillator was used to identify the ^{8}He particles since, for the same rigidity, they have twice the energy of the ^{4}He^{+1} particles. In Fig. 3 is shown an energy versus position two-dimensional display which has been gated by the ^{8}He^{+2} and ^{4}He^{+1} region depicted in Fig. 2. Transitions to the ground state of ^{16}Ne and a first excited state at 1.69 ± 0.07 MeV are clearly present, with the ground state counts corresponding to a laboratory differential cross section of 5 ± 3 nb/sr. (The error in the cross section reflects uncertainties in the target thickness, efficiency in the time-

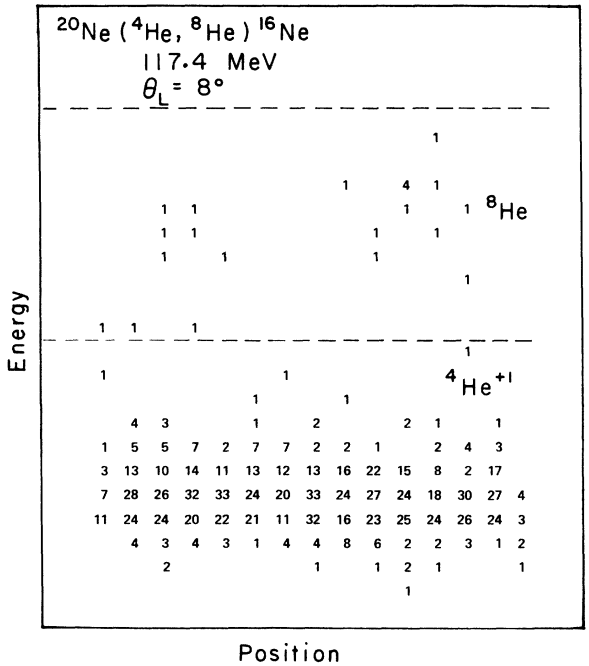

FIG. 3. Energy vs position two-dimensional display for the ^{20}Ne(^{4}He,^{8}He)^{16}Ne reaction, gated by time-of-flight and differential energy loss as depicted in Fig. 2. The ^{8}He^{+2} particles are separable from the ^{4}He^{+1} particles only in this display. The dashed line indicates the location of the ^{8}He gate.

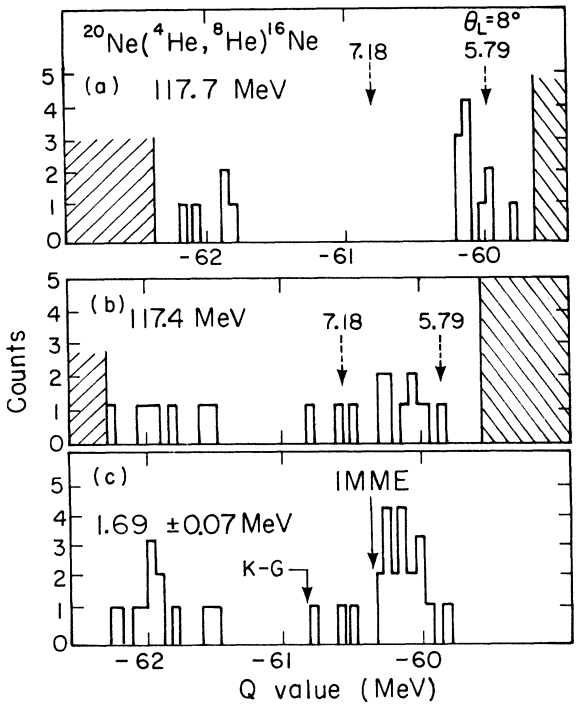

FIG. 4. (a) ^{8}He-gated position spectrum from the ^{20}Ne(^{4}He,^{8}He)^{16}Ne reaction at 117.7 MeV incident energy. The dashed arrows indicate the locations of strong inelastic states (see text) and the cross-hatched regions indicate the detector limits. (b) As in (a) but at 117.4 MeV. These are the data of Figs. 2 and 3. Note the shift in abscissa due to different spectrometer field settings at the two energies. (c) A kinematically-corrected sum of (a) and (b). Predictions of the ground state mass from both the IMME and Kelson-Garvey (K-G) approach are indicated by arrows.

zero detector, and statistical uncertainties.)

Projections of the ^{8}He position spectra from both experiments are shown in Fig. 4, with Fig. 4(b) corresponding to the data from Figs. 2 and 3. As mentioned earlier, the ^{4}He inelastic scattering was incident on the focal plane detector. In particular, at the beam energy of 117.7 MeV a state at 5.79 MeV and a possible doublet at 7.17 and 7.19 MeV excitation energy in ^{20}Ne were particularly intense. As shown in Fig. 4(a), the ground state of ^{16}Ne was located at the same focal plane location as the 5.79 MeV state. To ensure that the ^{16}Ne ground state was correctly identified and to obtain better statistics, the experiment was repeated at a beam energy of 117.4 MeV. As shown in Fig. 4(b), this moved the transitions to the ^{16}Ne ground state to a region between the two inelastic groups. The kinematically corrected sum spectrum is shown in Fig. 4(c). The ground state assignment is further reinforced by the observation of the first excited state of ^{16}Ne at 1.69 ± 0.07 MeV, which agrees well with the excitation energy of the first excited state of its mirror nucleus ^{16}C (1.75 MeV).[9]

The ground state Q value for the ^{20}Ne(^{4}He,^{8}He) ^{16}Ne reaction is −60.15 ± 0.08 MeV, which corresponds to a ^{16}Ne mass excess of 23.92 ± 0.08 MeV. The error associated with this mass assignment was obtained by adding in quadrature the effect that each of the uncertainties discussed in Sec. II has on the resulting ^{16}Ne mass. These errors are shown explicitly in Table I. This mass assignment agrees relatively well with, but is more accurate than, the mass excess of 24.4 ± 0.5 MeV which was recently obtained with the ^{16}O(π^+,π^-)^{16}Ne reaction.[12] The center-of-mass width of the ground state is 200 ± 100 keV as measured in our experiment; this was obtained by comparing the peak widths produced by the (^{4}He,^{4}He) and (^{4}He, ^{6}He) reactions to that from the (^{4}He,^{8}He) reaction.

B. ^{16}O(^{4}He,^{8}He)^{12}O

Immediately upon obtaining the spectrum shown in Fig. 4(b) in the second of the ^{16}Ne experiments, the ^{20}Ne target gas was replaced with ^{16}O and an attempt was made to measure the mass of ^{12}O. The Q value for the (^{4}He,^{8}He) reaction on ^{16}O is about 6 MeV more negative than on ^{20}Ne and, as shown in Fig. 5, the energy signal from the plastic scintillator did not produce as clean a separation as in the case of ^{16}Ne. However, there is evidence for a group of seven counts near the location of the IMME prediction for the ^{12}O ground

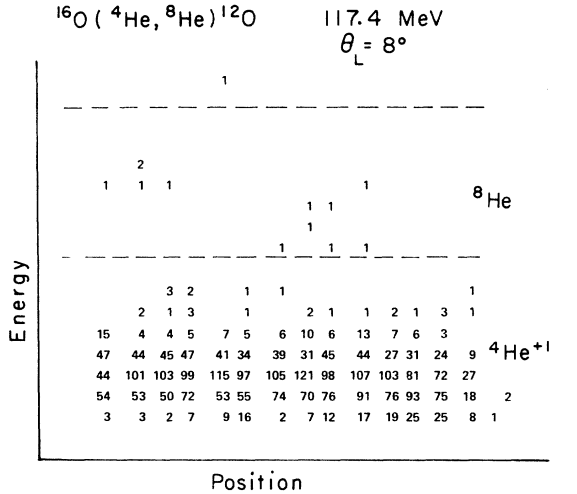

FIG. 5. Position vs energy two-dimensional display for the ^{16}O(^{4}He,^{8}He)^{12}O reaction gated by time-of-flight and differential energy loss regions set to include the ^{8}He^{+2} and ^{4}He^{+1} particles. The dashed line indicates the location of the ^{8}He gate.

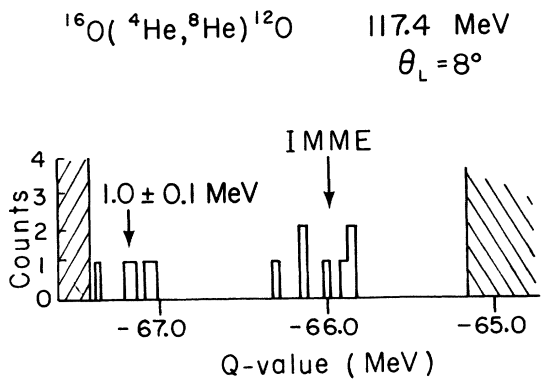

FIG. 6. ^{8}He-gated position spectrum obtained from the ^{16}O(^{4}He, ^{8}He)^{12}O reaction, which results from a projection of the data of Fig. 5. Cross-hatched regions indicate the limits of the detector. The IMME prediction for the ground state mass is indicated by an arrow.

state as well as five counts which could represent transitions to a first excited state. A projection of the ^{8}He particles onto the position axis is shown in Fig. 6. The seven ground state counts correspond to a laboratory differential cross section of 2 ± 1 nb/sr and a reaction Q value of -66.02 ± 0.12 MeV. (See Table I for a summary of the error analysis.) This Q value implies a mass excess of 32.10 ± 0.12 MeV for ^{12}O. Since the five counts comprising the first excited state are located near the end of the detector, a portion of this state could be cut off. The existing counts imply an excitation energy of 1.0 ± 0.1 MeV.

It is interesting to compare the results of the present reaction with those of reactions leading to states in ^{12}Be, the mirror nucleus of ^{12}O. A ^{7}Li(^{7}Li, $2p$)^{12}Be reaction study produced evidence for transitions to the g.s. as well as to a first excited state at 0.81 MeV.[20] The reactions ^{14}C (^{18}O, ^{12}Be)^{20}Ne (Ref. 21) and ^{10}Be(t,p)^{12}Be (Ref. 22) have located the ^{12}Be g.s. and an excited state at ~2.1 MeV but show no evidence for a state near 1.0 MeV. The spin and parity assignment for the 2.1 MeV state was established as 2^+ by means of the particle γ-ray angular correlation technique in the ^{10}Be(t,p)^{12}Be reaction. However, it has been postulated that the first excited state of ^{12}Be could be a 0^+ state near 2.2 MeV with the first 2^+ state at 4.3 MeV.[23] The 0^+ state would be formed from two nucleons occupying a depressed $2s_{1/2}$ orbital which is necessary to explain the $\frac{1}{2}^+$ ground state of ^{11}Be. Since the experimental value for the excitation energy of the 2^+ state is considerably lower than the predicted energy, it is possible that the proposed 0^+ state might be similarly lowered to near 1 MeV excitation energy. Although no corresponding $T = 2$ state has been found in ^{12}C or ^{12}B,[24] the evidence for a possible state near 1 MeV raises intriguing doubts as to the location of the first excited state which can only be resolved by further experiments.

C. ^{20}Ne(^{3}He,^{8}Li)^{15}F

Upon completion of the ^{16}Ne mass measurement, it was still necessary to determine the mass excess and ground state width of ^{15}F to ascertain whether ^{16}Ne decays by prompt diproton emission or by sequential proton decay through ^{15}F. A preliminary experiment by the MSU group at 75 MeV incident energy had produced evidence of a narrow peak near the Kelson-Garvey prediction for the location of the ^{15}F ground state. (A more complete account of the MSU experiment can now be found in Ref. 13.) We repeated this experiment at 87.8 MeV incident energy and 9° in the laboratory and produced the spectrum shown in Fig. 7(a). A narrow peak is evident near the Kelson-Garvey prediction for the ^{15}F ground state with a laboratory differential cross section of 80 ± 25 nb/sr. The peak located near channel 200 corresponds to transitions to the first excited state of ^{8}Li and the continuum below channel 200 arises from three body breakup.

In this reaction, however, it is also possible that the observed narrow peak could arise from transitions to the first excited state of ^{15}F with the yield of the ground state being much weaker.

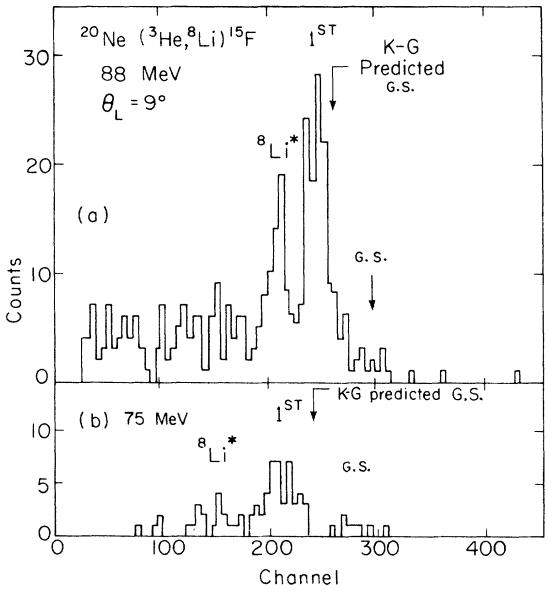

FIG. 7. (a) ^{8}Li-gated position spectrum obtained for the ^{20}Ne(^{3}He, ^{8}Li)^{15}F reaction at 87.8 MeV. The continuum below the ^{8}Li* peak is due to three-body breakup. (b) As in (a) but at 75.4 MeV incident energy. At the lower energy the weak g.s. transition is clearly visible.

This concern arises if one notes that the mirror nucleus ^{15}C has a ground state with $J^\pi = \frac{1}{2}^+$ and a first excited state at 0.74 MeV with $J^\pi = \frac{5}{2}^+$.[8] Therefore, nuclear structure considerations could argue for a dominant transition strength to a $\frac{5}{2}^+$ state if this were a simple pickup reaction.

As an approach toward determining the expected relative populations of the $\frac{1}{2}^+$ and $\frac{5}{2}^+$ states, the ^{22}Ne(^{3}He, ^{8}Li)^{17}F reaction was also investigated, since the ground and first excited state of ^{17}F have $J^\pi = \frac{5}{2}^+$ and $\frac{1}{2}^+$, respectively. In this case, the $\frac{5}{2}^+$ state was populated with 10 times the strength of the $\frac{1}{2}^+$ state. Based upon this comparison we have assumed that the strong, narrow peak in Fig. 7(a) arises from transitions to the $\frac{5}{2}^+$ first excited state in ^{15}F and that the weak yield at higher energy corresponds to transitions to the ground state. In order to further check this assumption, and to investigate the contributions of target contaminants, a second spectrum was taken at a beam energy of 75.4 MeV and $\Theta_L = 9°$ and is shown in Fig. 7(b). At this lower beam energy, transitions to the ground state are clearly observed with a laboratory differential cross section of 8 ± 4 nb/sr. The observed Q value of the ground state transition of -29.73 ± 0.18 MeV (see Table I for error analysis) corresponds to a mass excess of 16.67 ± 0.18 MeV for ^{15}F. The excitation energy of the first excited state, 1.3 ± 0.1 MeV, is 500 keV higher than the excitation energy of the first excited state in the mirror nucleus ^{15}C, presumably due to a Thomas-Ehrman shift of the probable $\frac{1}{2}^+$ ground state.[25] The center-of-mass widths of the ground and first excited states were 0.8 ± 0.3 MeV and 0.5 ± 0.2 MeV, respectively, and were determined by comparing peak widths from the ^{20}Ne(^{3}He, ^{8}Li)^{15}F reaction to those from the ^{22}Ne(^{3}He, ^{8}Li)^{17}F and ^{20}Ne(^{3}He, ^{6}Li)^{17}F reactions.

IV. DISCUSSION

The results of the present experiment are summarized in Table II. Also included are the results of similar experiments producing $T_z = -2$ and $-\frac{3}{2}$ nuclei in the same mass region. One trend observed in these results is that the Kelson-Garvey approach predicts most of these proton-rich nuclei to have higher mass excesses than are observed. Masses of nuclei with $A \leq 16$ are consistently overestimated by from 0.4 to 1.0 MeV. This disagreement might be expected to occur in these light nuclei and could be caused by incomplete cancellation of the Coulomb repulsion contributions to the binding energies, as calculated in the Kelson-Garvey approach, due to shell closure effects. This lack of cancellation should be most pronounced in ^{12}O and ^{15}F, but should also be present to some extent for ^{8}C, ^{13}O, and ^{16}Ne. These trends appear to be substantiated by the data of Table II.

With the measurement of the masses of the ground and first excited states of ^{12}O, ^{15}F, and ^{16}Ne the masses of all but one of the members of the $A = 12$ and 16 isospin quintets and the $A = 15$

TABLE II. Experimental mass excesses and widths of $T_z = -2$ and $-3/2$ light nuclei.

Nuclide	Experimental mass excess (keV)	Kelson-Garvey prediction (keV)	1p binding energy (keV)	2p binding energy (keV)	$\Gamma_{c.m.}$ (g.s.) (keV)	d [a] (keV)
			$T_z = -2$ nuclei			
^{8}C	35 100 ± 30 [b]	35 770	130 ± 110	−2150 ± 30	230 ± 50 [b]	6.5 ± 2.2
^{12}O	32 100 ± 120	33 050	100 ± 180	−1820 ± 120	400 ± 250 [c]	0 ± 11
^{16}Ne	23 920 ± 80	24 668	40 ± 200	−1330 ± 80	200 ± 100	8 ± 5
^{20}Mg	17 570 ± 30 [d]	17 400	2650 ± 30	2330 ± 30	•••	−2.3 ± 1.8
			$T_z = -\frac{3}{2}$ nuclei			
^{11}N	(24 920 ± 110) [e]	25 450	(−1930 ± 110)	(2070 ± 110)	(1500 ± 700) [e]	•••
^{13}O	23 105 ± 10 [f]	23 520	1522 ± 10	2123 ± 10	•••	−0.5 ± 2.3
^{15}F	16 670 ± 180	17 610	−1370 ± 180	3250 ± 180	800 ± 300	•••
^{17}Ne	16 480 ± 30 [f]	16 630	1500 ± 30	950 ± 30	•••	4.8 ± 5.6

[a] The d coefficients for $T_z = -2$ nuclei were calculated using the mass excesses of the 0^+, $T = 2$ states in the $T_z = -2$, 0, 1, and 2 nuclei. See Refs. 1, 6–10.

[b] Mass excess and natural width of ^{8}C are weighted averages of results of Refs. 1 and 6.

[c] Because of the poor statistics in the ^{12}O ground state the width is only an estimate.

[d] Mass excess of ^{20}Mg from Ref. 2.

[e] "Experimental" mass excess of ^{11}N is an IMME prediction using the $\frac{1}{2}^+$, $T = \frac{3}{2}$ states in $T_z = -\frac{1}{2}$, $\frac{1}{2}$, and $\frac{3}{2}$ nuclei. See Refs. 7–10, and 24. The ground state width was calculated as discussed in the text.

[f] Mass excess from Ref. 10.

TABLE III. Isobaric multiplet mass equation coefficients (keV).

Multiplet	J^π, T	a	b	c	d	χ^2
			Ground state [a]			
$A=12$	0^+, 2	27610±18	−1769±26	239±15		0.0
		27611±20	−1770±40	239±15	0±11	•••
$A=15$	$\frac{1}{2}^+$, $\frac{3}{2}$	12800±23	−2266±60	209±30		•••
$A=16$	0^+, 2	17983±3	−2584±12	216±8		2.8
		17984±3	−2587±13	206±10	8±5	•••
			First excited state [b]			
$A=15$	$\frac{5}{2}^+$, $\frac{3}{2}$	13799±25	−2453±60	220±30		•••
$A=16$	2^+, 2	19772±10	−2591±17	209±10		6.3
		19785±11	−2604±17	187±13	15±6	•••

[a] Ground state mass excesses taken from Ref. 10.
[b] Excitation energies for the first $\frac{5}{2}^+$, $T=\frac{3}{2}$ state in mass 15 and the first 2^+, $T=2$ state in mass 16 were taken from Refs. 8 and 9.

isospin quartet are known. Coefficients for quadratic and cubic fits to the mass 12, 15, and 16 multiplets are presented in Table III for the ground state and for the $A=15,16$ first excited states. The values of χ^2 obtained for the quadratic fits to the mass 12 and 16 ground states and the mass 16 first excited state imply that the IMME is working reasonably well in this mass region even though ^{12}O and ^{16}Ne are unbound. However, for mass 16 a nonzero cubic term is obtained outside of the experimental errors for both the ground and first excited state. In this respect the mass 16 quintet appears to be similar to the mass 8 quintet which, as shown in Table II, also produces a positive d coefficient.[1,6] No d coefficient is necessary for mass 12 within the experimental errors which have been obtained. Given the relatively few nucleons involved in these multiplets and the likelihood of Thomas-Ehrman shifts in the low-lying configurations, such a variation in the d coefficients appears reasonable.[1,5,6,26]

In Table IV the locations of the still unobserved first and second $T=2$ states in ^{16}F and $T=\frac{3}{2}$ states in ^{15}O and the lowest $T=2$ state in ^{12}N have been calculated using the coefficients of Table III.

TABLE IV. Predicted states.

Nuclide	J^π	T	Excitation energy (keV) [a]
^{12}N	0^+	2	12290±20
^{15}O	$\frac{1}{2}^+$	$\frac{3}{2}$	11130±35
^{15}O	$\frac{5}{2}^+$	$\frac{3}{2}$	12230±40
^{16}F	0^+	2	10080±20
^{16}F	2^+	2	11870±30

[a] Based on IMME coefficients listed in Table III. Calculations for $A=12$ and 16 include the d coefficient.

Since the masses and ground state widths of ^{16}Ne and ^{15}F have been determined, the probabilities for proton and diproton decay from ^{16}Ne can be evaluated by calculating the decay width for each channel using the relation[27]

$$\Gamma_i = 2\gamma_i^2 P_i \ , \qquad (1)$$

where γ_i^2 is the reduced width for the emitted particle in the parent nucleus, P_i is the penetrability of the emitted particle through the combined Coulomb and centrifugal barriers, and Γ_i is the partial decay width for the process.

Since the ground states of ^{16}Ne and ^{15}F are both broad, ^{16}Ne is unbound to the emission of a single proton (see Fig. 8). Therefore the penetrability factor in Eq. (1) has been determined as a weighted average over all possible decay energies. The weighting assumes that the parent and daughter ground states possess Gaussian distributions and the diproton penetrability is calculated for a $Z=2$, $A=2$ particle incident on ^{14}O, at $R=4.77$ fm.

Assuming the Wigner limit for the reduced width in Eq. (1) and using the appropriately weighted proton and diproton penetrabilities, we obtain a total decay width for ^{16}Ne of 20 keV (the experimental width is 200±100 keV) and a diproton branching ratio of 20%. Consideration of the uncertainties in the masses and widths leads to the total decay width varying from 5 to 100 keV and a diproton branching ratio of 10 to 90%.

In order to perform a similar calculation for the decay of ^{12}O, it is necessary to estimate the mass and ground state width of ^{11}N, since only its $\frac{1}{2}^-$ first excited state is known.[28] The ^{11}N

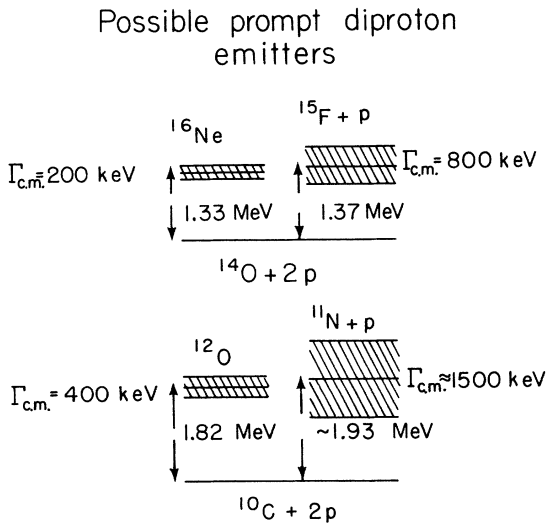

FIG. 8. Energies of the two possible prompt diproton emitters ^{16}Ne and ^{12}O. The binding energies and ground state widths are taken from Table II. Cross-hatched regions represent the full width at half maximum of the ground states.

ground state mass may be estimated using the IMME (see Table II). Since the width of its first excited state is known to be 740 ± 100 keV, a very rough approximation for the ground state width relative to that for the first excited state may be obtained by evaluating the relative penetrabilities of the $l = 0$ protons from the $\frac{1}{2}^+$ ground state and the $l = 1$ protons from the $\frac{1}{2}^-$ first excited state. This calculation results in a ground state width for ^{11}N of 1.5 ± 0.7 MeV with the error being an estimate as to the reliability of the calculation. Using this estimated mass and width for ^{11}N, and again assuming the Wigner limit for the reduced widths, a total decay width for ^{12}O of 0.2 to 1.2 MeV (the experimental width is estimated to be 0.40 ± 0.25 MeV) and a diproton branching ratio of 30 to 90% are obtained.

Since the Wigner limit has been assumed, the above results should represent an upper limit for the diproton branching ratios from ^{16}Ne and ^{12}O. A more realistic estimate of the diproton reduced width, obtained by projecting out (via Moshinsky brackets)[29] a diproton cluster, assuming a simple $(1d_{5/2})^2_{0^+}$ proton configuration for ^{16}Ne and a $(1p_{1/2})^2_{0^+}$ configuration for ^{12}O, leads to branching ratios of 3% and 6% for the diproton decays of ^{16}Ne and ^{12}O, respectively.

In conclusion, the masses of the unbound nuclides ^{16}Ne, ^{15}F, and ^{12}O have been measured and are found to agree well with predictions of the isobaric multiplet mass equation. Based on the measured masses, penetrability calculations suggest that both ^{16}Ne and ^{12}O should have significant branching ratios for prompt diproton decay. Although considerable experimental effort will be required in order to distinguish between diproton decay and sequential proton emission from these nuclei, it would appear from our experimental results and these calculations that the early prediction[14] of the unique diproton decay patterns of ^{16}Ne and ^{12}O will be substantiated.

Note added in proof. Our values for the mass excess and width of the ^{15}F g.s. agree well with the results in Ref. 13, which became available subsequent to the completion of our paper. Good agreement is also found for the ^{15}F first excited state, with the exception that the width reported in Ref. 13, 240 ± 30 keV, is somewhat narrower than our determination. Possibly this is related to an underestimate of our experimental resolution for the (^{3}He, ^{8}Li) reaction.

V. ACKNOWLEDGMENTS

The authors would like to acknowledge the efforts of B. G. Harvey and J. Mahoney in designing and constructing the versatile focal plane detector used in these experiments, G. Gabor for his assistance in designing the time-zero detector, Kumar Ganguly for his help with the early stages of this experimental project, and D. Hendrie for many useful discussions. This work was performed under the auspices of the U. S. Energy Research and Development Administration.

*Present address: Williams College, Williamstown, Massachusetts 01267.
‡On leave from Institut für Strahlen-und Kernphysik Bonn, Universität Bonn, West Germany.

[1]R. E. Tribble, R. A. Kenefick, and R. L. Spross, Phys. Rev. C 13, 50 (1976).
[2]R. E. Tribble, J. D. Cossairt, and R. A. Kenefick, Phys. Lett. 61B, 353 (1976).
[3]R. E. Tribble, J. D. Cossairt, and R. A. Kenefick, Phys. Rev. C 15, 2028 (1977).
[4]W. Benenson, A. Guichard, E. Kashy, D. Mueller, H. Nann, and L. W. Robinson, Phys. Lett. 58B, 46 (1975); W. Benenson, D. Mueller, E. Kashy, H. Nann, and L. W. Robinson, Phys. Rev. C 15, 1187 (1977).
[5]E. P. Wigner, in *Proceedings of Robert A. Welch Foundation Conferences on Chemical Research, Houston, Texas, 1957*, edited by W. O. Milligan (Robert A. Welch Foundation, Houston, Texas, 1957), p. 67.
[6]R. G. H. Robertson, W. Benenson, E. Kashy, and D. Mueller, Phys. Rev. C 13, 1018 (1976).
[7]F. Ajzenberg-Selove, Nucl. Phys. A248, 1 (1975).
[8]F. Ajzenberg-Selove, Nucl. Phys. A268, 1 (1976).

[9]F. Ajzenberg-Selove, Nucl. Phys. A281, 1 (1977).
[10]A. H. Wapstra and K. Bos, At. Data Nucl. Data Tables 17, 474 (1976).
[11]I. Kelson and G. T. Garvey, Phys. Lett. 23, 689 (1966).
[12]R. J. Holt, B. Zeidman, D. Malbrough, T. Marks, B. Preedom, M. Baker, R. Burman, M. Cooper, R. Heffner, D. Lee, R. Redwine, and J. Spencer, Phys. Lett. 69B, 55 (1977).
[13]W. E. Benenson, Mich. State Univ., private communication; W. Benenson, E. Kashy, A. G. Ledebuhr, R. C. Pardo, R. G. H. Robertson, and L. W. Robinson, following paper, Phys. Rev. C 17, 1939 (1978).
[14]V. I. Goldanski, Zh. Eksp. Teor. Fiz. 39, 497 (1960) [Sov. Phys.–JETP 12, 348 (1961)]; Nucl. Phys. 19, 482 (1960).
[15]H. Stelzer, Nucl. Instrum. Methods 133, 409 (1976).
[16]G. KeKelis and G. Gabor, Lawrence Berkeley Laboratory Annual Report No. LBL-5075, 1975 (unpublished), p. 352.
[17]D. L. Hendrie, J. R. Meriwether, F. Selph, D. Morris, and C. Glashausser, Bull. Am. Phys. Soc. 15, 650 (1970).
[18]B. G. Harvey, J. Mahoney, and R. F. Burton, Lawrence Berkeley Laboratory Annual Report No. LBL-5075 1975 (unpublished), p. 354; H. Homeyer, J. Mahoney and B. G. Harvey, Nucl. Instrum. Methods 118, 311 (1974).
[19]A. D. Bacher, E. A. McClatchie, M. S. Zisman, T. A. Weaver, and T. A. Tombrello, Nucl. Phys. A181, 453 (1972).
[20]H. H. Howard, R. H. Stokes, and B. H. Erkkila, Phys. Rev. Lett. 27, 1086 (1971).
[21]G. C. Ball, J. G. Costa, W. G. Davies, J. S. Forster, J. C. Hardy, and A. B. McDonald, Phys. Lett. 49B, 33 (1974).
[22]D. E. Alburger, D. P. Balamuth, J. M. Lind, L. Mulligan, K. C. Young, R. W. Zurmühle, and R. Middleton, unpublished abstract.
[23]F. C. Barker, J. Phys. G 2, L45 (1976).
[24]D. Ashery, M. S. Zisman, G. W. Goth, G. J. Wozniak, R. B. Weisenmiller, and J. Cerny, Phys. Rev. C 13, 1345 (1976).
[25]A. M. Lane and R. G. Thomas, Rev. Mod. Phys. 30, 257 (1958).
[26]D. H. Wilkinson, Phys. Rev. Lett. 13, 571 (1964).
[27]J. B. Marion and F. C. Young, *Nuclear Reaction Analysis Graphs and Tables* (North-Holland, Amsterdam, 1966), p. 84.
[28]W. Benenson, E. Kashy, D. H. Kong-A-Siou, A. Moalem, and H. Nann, Phys. Rev. C 9, 2130 (1974).
[29]T. A. Brody and M. Moshinsky, *Tables of Transformation Brackets* (Gordon and Breach, New York, 1967).